# 私立東海大學

# 資訊工程研究所

# 碩士論文

指導教授：黃育仁 教授

間接性螢光抗核抗體顯影之自動檢測技術

Automatic Detection and Classification of Antinuclear Autoantibodies Cells in Indirect Immunofluorescence Images

研究生：江艾珊

中　華　民　國　九　十　九　年　七　月

# 摘要

在組織性自我免疫的疾病中，目前最受大家推薦用來檢測抗核抗體(antinuclear autoantibody, ANA)的方法是利用 HEp-2 的間接性螢光切片進行檢查。而此動作需要檢驗人員透過顯微鏡觀察細胞切片的形狀，才能夠進行完整且詳盡的定義。然而，因為缺乏自動化的檢驗流程及標準化的作業程序，此一檢驗過程仍然需要在專業且具有相當經驗的醫師或技術人員的指導下，才能獲得精確的診斷結果。因此在這樣的環境下，本論文的研究目的在於提出一個針對 ANA 進行自動檢驗的系統。此系統可以分為兩大部分，包含細胞偵測與影像分類。研究的第一部分是在間接性螢光切片的影像中，自動偵測出螢光性樣本中各細胞的邊緣與外型，並且利用針對圓進行霍夫轉換的技術，對於系統所找到的細胞進行初步的判斷。研究的另一個部分則是利用影像中的各個特徵，結合決策樹的方法對於影像進行分類。本論文針對六種抗核抗體類型的影像進行研究，而研究結果證明此方法提供一個穩定且快速的系統用於間接抗體螢光染色 HEp-2 細胞的偵測與分類。

**關鍵字**：間接性螢光切片、抗核抗體、組織性自我免疫、細胞偵測、影像分類

# ABSTRACT

Indirect immunofluorescence (IIF) with HEp-2 cells presents the major screening method for detection of antinuclear autoantibodies (ANA) in systemic autoimmune diseases. The identification of patterns has recently by a human inspecting the slides with a microscope. However, due to lacking in satisfied automation of inspection and a low level of standardization, this procedure still need highly specialized and experienced technician/physician to obtain diagnostic result. For this purpose, the aim of this paper is for developing an automatic inspection system that can be divided into HEp-2 cell detection and fluorescence pattern classification in ANA testing. The first part of this study is an automatic detection scheme to sketch outlines of fluorescence cells for HEp-2 cell detection in the IIF images by using the circular Hough transform (CHT). The second part of the system uses a decision tree for image classification of fluorescence pattern by using ANA characteristics. This study evaluates cells with six distinct fluorescence patterns from ANA images. The simulation results show that the proposed method provides a robust and fast automatic detection and classification of HEp-2 fluorescent patterns in ANA testing.



***Keywords***: indirect immunofluorescence pattern, antinuclear autoantibodies, systemic autoimmune diseases, cell detection, image classification

# INDEX

# LIST OF TABLES

# LIST OF FIGURES

# CHAPTER1

# INTRODUCTION

Antinuclear antibodies (ANA) are defined as those recognizing antigens morphologically confined to the cell nucleus. Detection of ANA is a common marker in patients with suspected connective tissue diseases, and the recommended method for ANA testing is the indirect immunofluorescence (IIF) imaging [1-3]. IIF image with HEp-2 cells is used for the detection of ANA in systemic autoimmune diseases [4]. The IIF slides are examined at the fluorescence microscope, and physicians report both the estimation of fluorescence intensity and the description of staining pattern. However, due to lacking in satisfied automation of inspection and a low level of standardization [5;6], this procedure still needs highly specialized and experienced technician or physician to obtain diagnostic result [7]. Consequently, automatic inspection for fluorescence patterns in IIF image may assist physicians, without relevant experience, in making rapid and correct diagnosis.

With ANA testing are now in widespread use, a automatic inspection system is becoming essential and urgent for its clinical application [8]. In the past years, there were many methods about IIF image with HEp-2 cells have been presented [9-12]. However, these methods differ widely and are mostly not specified [13]. To improve these situations, this paper provided the method which was different from others. The

aim of this thesis was for developing an automatic inspection system that could be divided into HEp-2 cell detection and fluorescence pattern classification in ANA testing. The first part of this study was that it used the technology of circular Hough transform (CHT) for an automatic detection scheme to sketch outlines of fluorescence patterns with HEp-2 cell detection in the IIF images. The CHT, a reliable unsupervised model, is applied to solve diverse image detection problems. The results of computer simulations revealed that the proposed method always identified cell outlines as were obtained by manual sketched. The proposed automatic detection system could save much of the time required to locate fluorescence patterns with very high stability. After detecting HEp-2 cells in ANA testing, this study proposed a classification scheme based on a decision tree classifier with four features to identify fluorescence patterns. The features included gray-level threshold, Euler number, disorders and ratio of cell gray-level. The result showed that these features are useful for fluorescence pattern classification.

The rest of this paper is organized as follows. Chapter 2 presents the proposed methods and shows the experiment results. Chapter 3 discusses the classification for the IIF images. The conclusion follows in chapter 4.

# CHAPTER2

# CELL DETECTION

## 2.1 DATA ACQUISITION

This study used slides of HEp-2 substrate, at a serum dilution of 1:80. A physician takes images of slides with an acquisition unit consisting of the fluorescence microscope coupled with a commonly used fluorescence microscope (Axioskop 2, CarlZeiss, Jena, Germany) at 40-fold magnification. The immunofluorescence images were taken by an operator with a color digital camera (E-330, Olympus, Tokyo, Japan). The digitized images were of 8-bit photometric resolution for each RGB (Red, Green and Blue) color channel with a resolution of 3136×2352 pixel. Finally, the images were transferred to a personal computer and stored as *.orf-files (Raw data format) without compression. The image database containing 113 samples were collected from January 2008 to July 2008. Due to the size of original images was too large to adapt a detection procedure, thus this study down-sampled the image to a reasonable resolution 1024×768 pixel.

## 2.2 AUTOANTIBODY FLUORESCENCE PATTERNS

There are more than thirty different nuclear and cytoplasmic patterns can be identified, which are given by upward of 100 different autoantibodies [14]. In the

analysis, such patterns are typically grouped in the following classes [15], [16] that are specific to the most relevant and recurrent ANA:

1) Diffuse pattern: diffuse staining of the interphase nucleolar and staining of the chromatin of mitotic cells

2) Peripheral pattern: solid staining, primarily around the outer region of the nucleus, with weaker staining toward the center of the nucleus

3) Speckled pattern: a fine or coarse granular nuclear staining of the interphase cell nucleolar (fine speckled pattern, coarse speckled pattern and discrete speckled pattern)

4) Nucleolar pattern: large coarse speckled staining within the nucleus, less than six in number per cell

To evaluate the proposed system, the IIF image database included six primary ANA patterns: diffuse pattern, peripheral pattern, coarse speckled pattern, fine speckled pattern, discrete speckled pattern, and nucleolar pattern. Figures 1 illustrates the relation of the six main ANA patterns. Under the observation, the fluorescence cell belongs to diffuse, peripheral, coarse speckled, or fine speckled pattern normally included only one connected region, but the discrete speckled and nucleolar patterns consisted of mass and several connected regions, respectively.

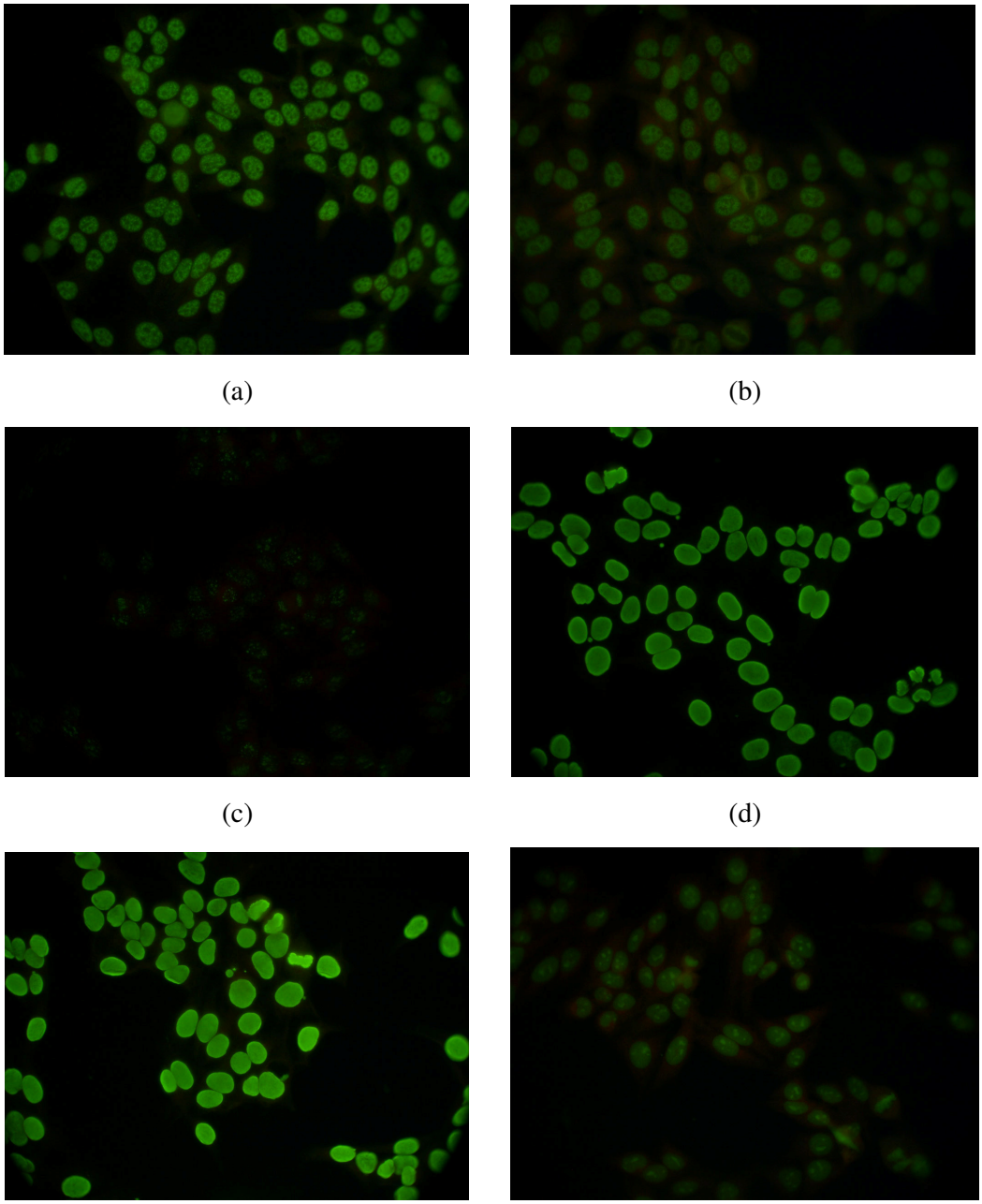

(a) (b)

(c) (d)

(e) (f)

Fig. 1. Types of ANA: (a) coarse speckled pattern, (b) fine speckled pattern, (c) discrete speckled pattern, (d) peripheral pattern, (e) diffuse pattern and (f) nucleolar pattern.

## 2.3 AUTOMATIC DETECTION

One of the most reliable region-based methods of automatic and unsupervised detection is the watershed transformation [17]. This technique has been applied successfully to solve a wide range of difficult problems of image detection. Due to the variety of ANA patterns, the region-based methods always failed to detect cells of connected region cells in images. This paper provided the technique of circular Hough transform for detecting cells, it can successfully to solve a connected region cells problem in ANA testing. Figure 2 presents a flowchart of the proposed method in a form that includes the preprocessing and detection phases. This study performed pre-processing in ANA images firstly, for example, that cleared noises to avoid them interference a decision of a system. Then the system calculated an Euler number for each images because the shape of discrete pattern was different from other patterns. If it was not the discrete pattern, the proposed method separated each cells into two groups (sparse region cells or connected region cells) by calculating cell sizes in image, and the system used circular Hough transform to outline each shape of cells; otherwise the system might use a circular Hough transform to find each similar cell shapes. Finally, the proposed method could outline almost cell shapes in IIF images.

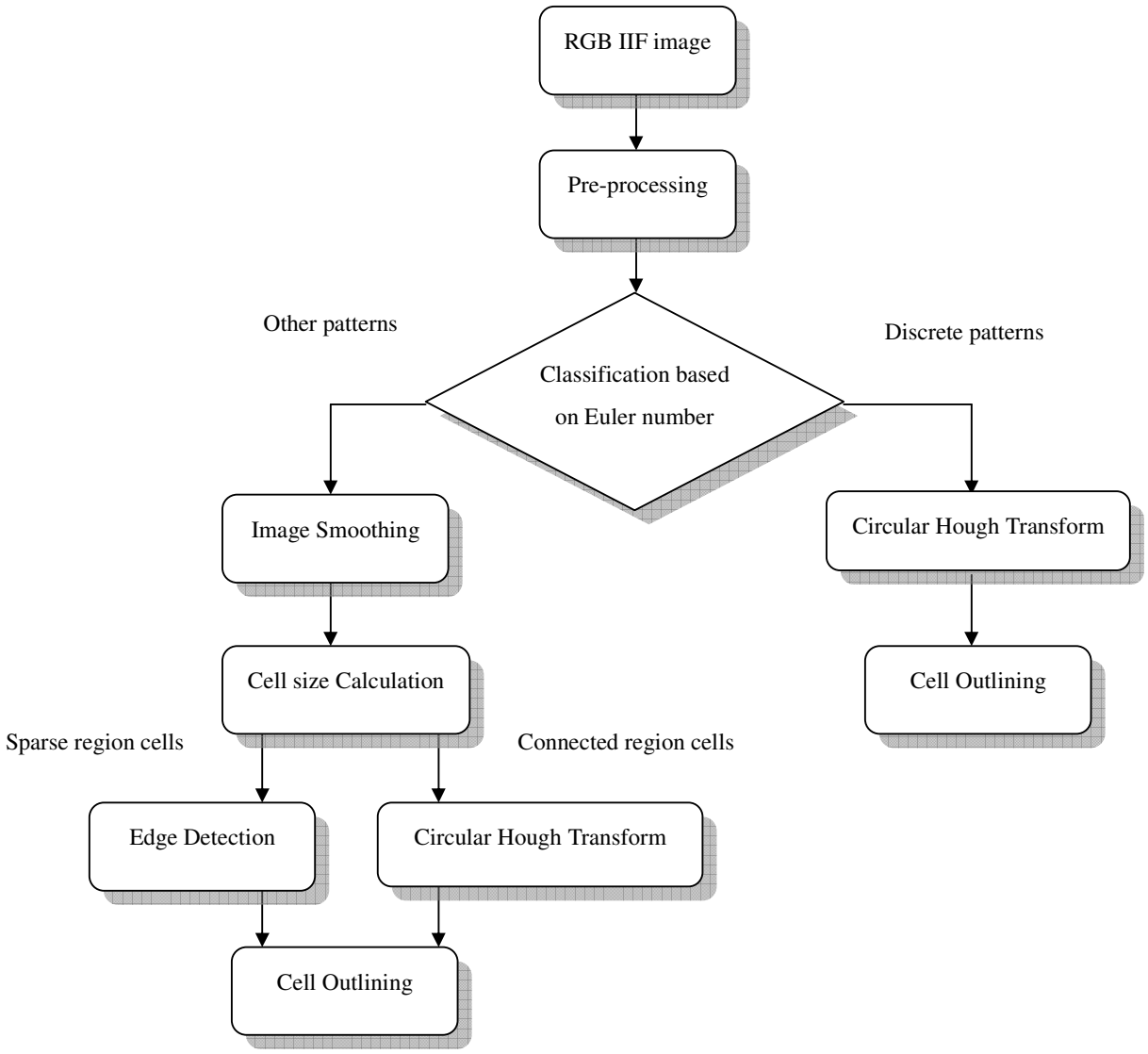


Fig. 2. The flowchart of the proposed method

## 2.4 PREPROCESSING OF THE PROPOSED METHOD

The Preprocessing is a significant step before the detection as IIF images include considerable noises and speckles that render detection difficult. The Wiener filter is one of the established linear filtering methods and widely known for its excellent

performance in de-noising a white noise [18]. The Wiener method is a pixel-wise adaptive low-pass filtering method based on statistics estimated from the local neighborhood of each pixel. Wiener filter performs well for images corrupted by additive noise. This study performed the practical filter, the Wiener method to enhance IIF images for HEp-2 cell outlining. The proposed method using the preprocessing not only reduced the number of speckles and the amount of noises in images but also preserved the shape and contrast of fluorescence patterns.

## 2.5 EULER NUMBER

Due to the discrete speckled pattern and other patterns have diverse shapes of the immunofluorescence areas, the cell outline of discrete speckled pattern would be damaged after Wiener method. Thus the proposed method performed a simple classifier to separate discrete speckled pattern from other types and then to adopt distinct preprocessing procedures. This study utilized the Euler number from an IIF image as a property to identify the discrete speckled pattern. In this paper, the RGB IIF images were transformed into gary-level firstly and then the images were converted to binary images using the automatic Otsu's thresholding algorithm [19]. Figure 3 shows the immunofluorescence areas in the cytoplasm of nucleolus for the discrete speckled pattern. The Euler number, a measure of the topology of an image,

is defined as the total number of objects in the image minus the number of holes in those objects [20]. Suppose that $E$ is Euler number, $C$ is the total number of objects in the image, and H is the number of holes in those objects. The $E$ (must be an integer) can be defined as

$$E = C - H \tag{1}$$

If Euler number of an IIF image was over 100, the image would be classified as discrete speckled pattern in this study.

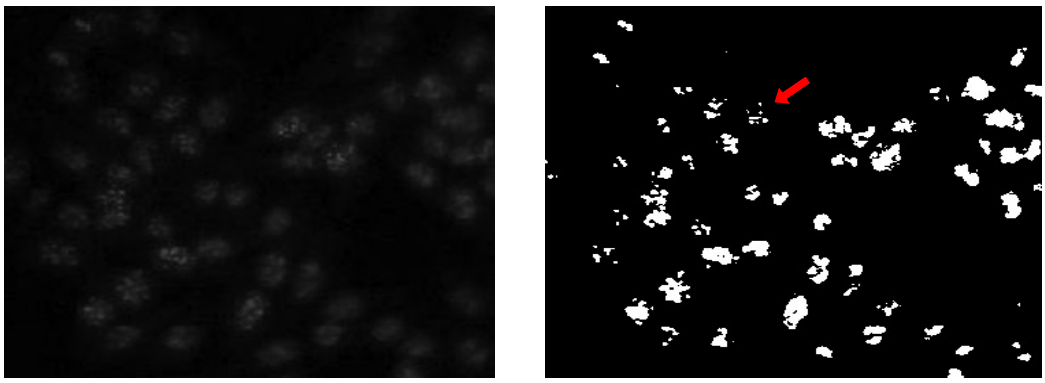

(a) (b)

Fig. 3. (a) a discrete speckled pattern image and (b) immuno-fluorescence areas in the cytoplasm of nucleolus.

For other five types (coarse speckled pattern, fine speckled pattern, discrete speckled pattern, peripheral pattern, diffuse pattern, and nucleolar pattern), the Wiener filter with 10 pixels radius was required for improving the performance of cell outlining.

## 2.6 CIRCULAR HOUGH TRANSFORM (CHT)

Due to cells in an IIF image might locate on top of another, this study separated the connected region cells for detecting their single shape by using the standard circular Hough transform (CHT) to detect circles in a binary image. The technique of CHT for the detection of a range of circle sizes, the use of orientation information, can each be expressed in terms of a convolution operator [21]. Assumed that $R$ is the radius of the largest circle and the considered convolution operator is orientation annulus *(OOA)* that it consists of a vector field containing two components, $OOA = (OOA\_X\ ,\ OOA\_Y\ )^T$. If the distance between $R$ and a point *(m, n)* conformed to a range of $R$, the value could be useful, otherwise it is zero.

$$O_{OA\_x}(m,n) = \begin{cases} \cos\theta_{mn} & if \quad R_{\min}{}^2 < m^2 + n^2 < R_{\max}{}^2 \\ 0 & otherwise \end{cases} \tag{3}$$

and

$$O_{OA\_y}(m,n) = \begin{cases} \sin\theta_{mn} & if \quad R_{\min}{}^2 < m^2 + n^2 < R_{\max}{}^2 \\ 0 & otherwise \end{cases} . \tag{4}$$

The CHT can be formulated as a convolution whose mask coefficients. The operator for the orientation annulus requires the dot product between the edge image gradients, and the vector field contained within the orientation annulus.

The convolution operators were applied to either an edge magnitude image $||E||$, where $E = (\ Ex\ ,\ Ey\ )^T$, the partial gradient images in $x$ and $y$ *(Ex and Ey, respectively)*.

Suppose that *(i, j)* is a single edge point, and *(x, y)* is a single accumulator point. The contribution output *Q* made to a single accumulator point:

$$Q_{OA}(x, y) = \sum_i \sum_j E^T(i, j) O_{OA}(x - i, y - j) \quad . \tag{5}$$

This paper swept over every edge point in the input image drawing circles with the desired radii and increasing the values in our accumulator. The accumulator contained numbers corresponding to the number of circles passing through the individual coordinates [22]. Then the system chose the core of the centers in circles as new centers if there were the highest numbers correspond to the center. By using the new center to sketch an adjusted circle, the sparse region cells shapes of connected region cells were outlined.

**2.7 RESULT**

This study totally experimented 7614 autoantibody fluorescence patterns with manual sketched outlines (including 620 diffuse patterns, 1077 peripheral patterns, 2251 coarse speckled patterns, 1509 fine speckled patterns, 852 discrete speckled patterns and 1305 nucleolar patterns) from 113 IIF images to test the accuracy of the proposed method. This work presented a practical detection method for automatically detecting outlines of fluorescence cells in IIF images. The preprocessing procedure enhanced IIF images and then the CHT was utilized to produce the outline of the cell

automatically.

The performance measures, i.e. accuracy and sensitivity, were used to estimate the performance of the proposed method. Table 1 lists the detection results of the proposed method. The system clearly yielded cell outlines that are similarly to those manually sketched. But there were various cases are mixed indeed. In these cases, serious overlapping could be found between the cells. Figure 4 shows the detection examples. From the detection results, only a small number of cases might generate an undesired detection.

Table 1 Fluorescence patterns detection performances of the proposed method

| Type of pattern | Image sample | Number of cell | Accuracy | Sensitivity |
|---|---|---|---|---|
| Coarse speckled | 30 | 2251 | 92.86% | 92.38% |
| Fine speckled | 20 | 1509 | 87.76% | 97.13% |
| Discrete speckled | 15 | 852 | 87.56% | 91.28% |
| Peripheral | 20 | 1077 | 85.51% | 90.17% |
| Diffuse | 8 | 620 | 81.49% | 92.27% |
| Nucleolar | 20 | 1305 | 89.82% | 94.90% |
| total | 113 | 7614 | 88.77% | 93.43% |

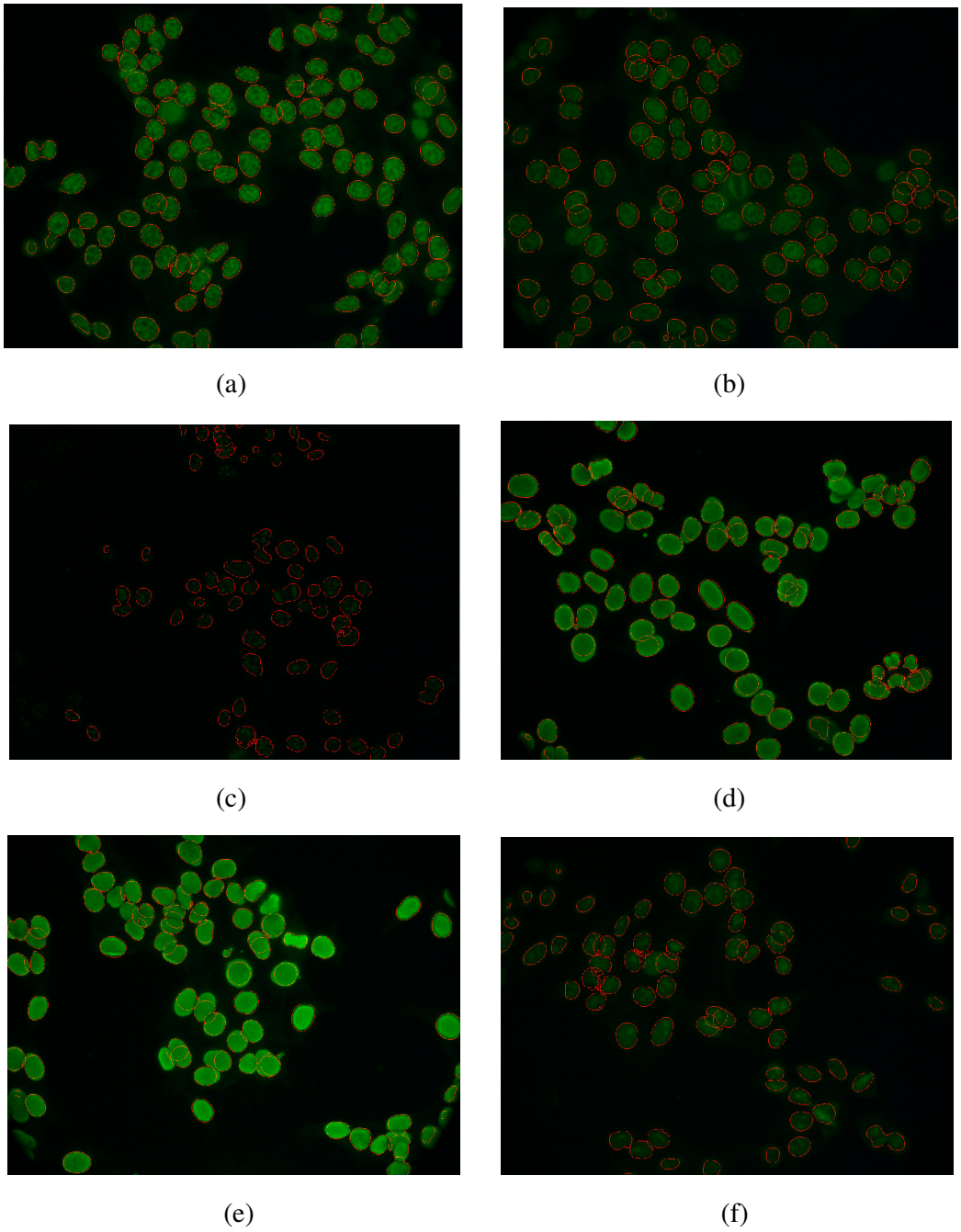


Fig. 4. The detection results: (a) coarse speckled pattern, (b) fine speckled pattern, (c) discrete speckled pattern, (d) peripheral pattern, (e) diffuse pattern and (f) nucleolar pattern

# CHAPTER3

# IMAGE CLASSIFICATION

Cells that are considered in the application for an automated image analysis are Hep-2 cells which are used for the identification of ANA [23]. Classification on HEp-2 cells could be divided into two intentions. The first part is to find unique features which the difference between the six fluorescence patterns. The second part is how to choose a useful classifier. In this study, the four features utilized to identify fluorescence patterns, which were the gray-level threshold, an Euler number, disorders and the ratio of cell gray-level. This system used decision tree to classify IIF images by above features. Finally, the proposed method could identify six distinct fluorescence patterns in IIF images.

## 3.1 FEATURE EXTRACTION

The texture of medical images is the main feature uses in pattern recognition and it relates with the appearance, structure and arrangement of the parts of an object. Texture is an important spatial feature useful for identifying objects or regions of interest in an image [24]. For example, if there are constants in image pixels, it shows that an image has not any textures; on the contrary, there are many textures in images. Many approaches are developed to extract the texture features of an image. Texture

analysis use radiological images obtained in routine diagnostic practice, but involve an ensemble of mathematical computations performed with the data contained within the images. The proposed method employed the previous contouring procedure to obtain outline of an IIF images. Four morphologic features from the extracted counter within images were performed to classify IIF images.

Gray-level threshold — A gray level tells about the brightness of a pixel within image recognition system [25]. The brightness is a positive integer value taken into better image quality for feature extraction. For an 8-bit gray level image, the feature extraction and object recognition outcomes result brightness ranges from 0 to 255, with 0 representing black from the quality image processing and 255 representing white. This proposed method counted a threshold in gray-level images. If the gray-level value of each pixel was bigger than the threshold, it might be its value; otherwise it might be zero. Then the system counted the ratio between original gray-level images and the result of classification using a threshold.

Euler number — The Euler number , a measure of the topology of an image, was defined as total number of objects in the image minus the number of holes in those objects. If Euler number of an IIF image was over 100, the image would be classified as discrete speckled pattern in this study. This paper also calculated the Euler number see Chapter 2.5.

Disorders — There were many textures of cell in gray-level images so this paper used standard deviation to count disorders of images. In probability theory and statistics, the standard deviation of a statistical population, a data set, or a probability distribution is the square root of its variance. The standard deviation remains the most common measure of statistical dispersion, measuring how widely spread the values in a data set are. If many data points are close to the mean, the standard deviation is small; if many data points are far from the mean, then the standard deviation is large. If all data values are equal, then the standard deviation is zero. The definitions for the standard deviation *s* of a data vector *X* and *n* is the number of elements:

$$s = \left[ \frac{1}{n-1} \sum_{i=1}^{n} \left( x_i - \bar{x} \right)^2 \right]^{\frac{1}{2}} \quad . \tag{6}$$

Ratio of cell gray-level — Gray-level is a series of achromatic tones having varying proportions of white and black, to give a full range of grays between white and black . The ratio of cell gray-level is the ratio of each degree of gray-level cells in IIF images. Figure 5 shows the example of the ratio of cell gray-level. There was two degree of gray-level in each cell, for example, the gray-level degree of speckled with coarse speckled pattern is lower than the cytoplasm in a cell.

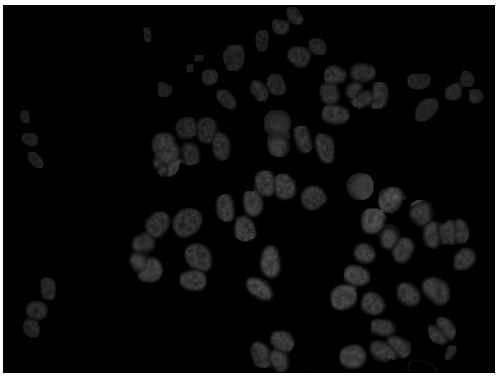

Fig. 5. The ratio between the degree of gray-level cell and each cell in image

This study calculated the four features from the entire volume area in images. These features were the fundamental and clinically useful indicators in the differential classes of IIF images. Eventually, this study gained four pattern indices for the areas in the HEp-2 cells after image analysis. This paper used decision tree with these features for pattern classification.

### 3. 2 PATTERN CLASSIFICATION

Image classification plays an important part in the fields of remote sensing, image analysis and pattern recognition [26]. A decision tree is one of the most popular classification algorithms used in data mining and machine learning to create knowledge structures that guide the decision making process [27]. This paper performed the practical classification, the decision tree induction algorithm to classify

IIF images for pattern recognition. The aim of decision tree was to separate an object into some groups. Scientists considered about the appearance from a group of orderless, ruleless instances for classification rule of decision tree. People provide an easy to read graphical presentation to decisions under considerations [28]. The architecture of decision tree consists of five main components: [29]

1) Decision Nodes: represented by squares that precede variables or actions that the decision-maker control

2) Chance Event Nodes: represented by circles that precede events that cannot be controlled

3) Terminal / End Nodes: end points where outcome values are attached

4) Decisions: branches out-coming from decision nodes; they represent alternative decisions available to decision-makers

5) Chance Outcome: branches out-coming from chance event nodes; they represent possible outcomes of decisions; they are assigned probability.

Figure 6 shows the structure of a decision tree. It presents a simple decision tree with two decisions and three chance events resulting from each decision. A tree has one root, normally a decision node, drawn chronologically from left to right; branches with decisions and outcomes are radial lines originated from the nodes. Common classification method of decision tree adapts top-down recursive mode to compare

attribute value in internal node that leads to conclusion at the root node of decision tree by judging downward branch from the node according to different attribute value [30].

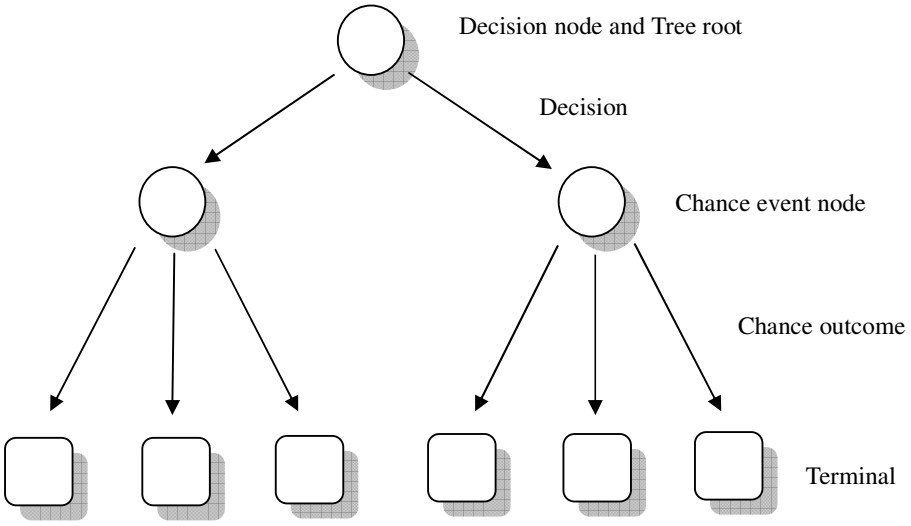


Fig. 6. The structure of a decision tree

This study used the basic theory of decision tree to classify six fluorescence patterns. Figure 7 presents a flowchart of the pattern classification that could be divided into two stages. The first step used threshold of gray-level images to separate three groups (nucleolar and discrete speckled, fine speckled and diffuse, peripheral and coarse speckled). Each group might choose a useful texture to classify, for example, this thesis used an Euler number to separate nucleolar and discrete speckled. Finally, the proposed method could identify six distinct fluorescence patterns in IIF

images.

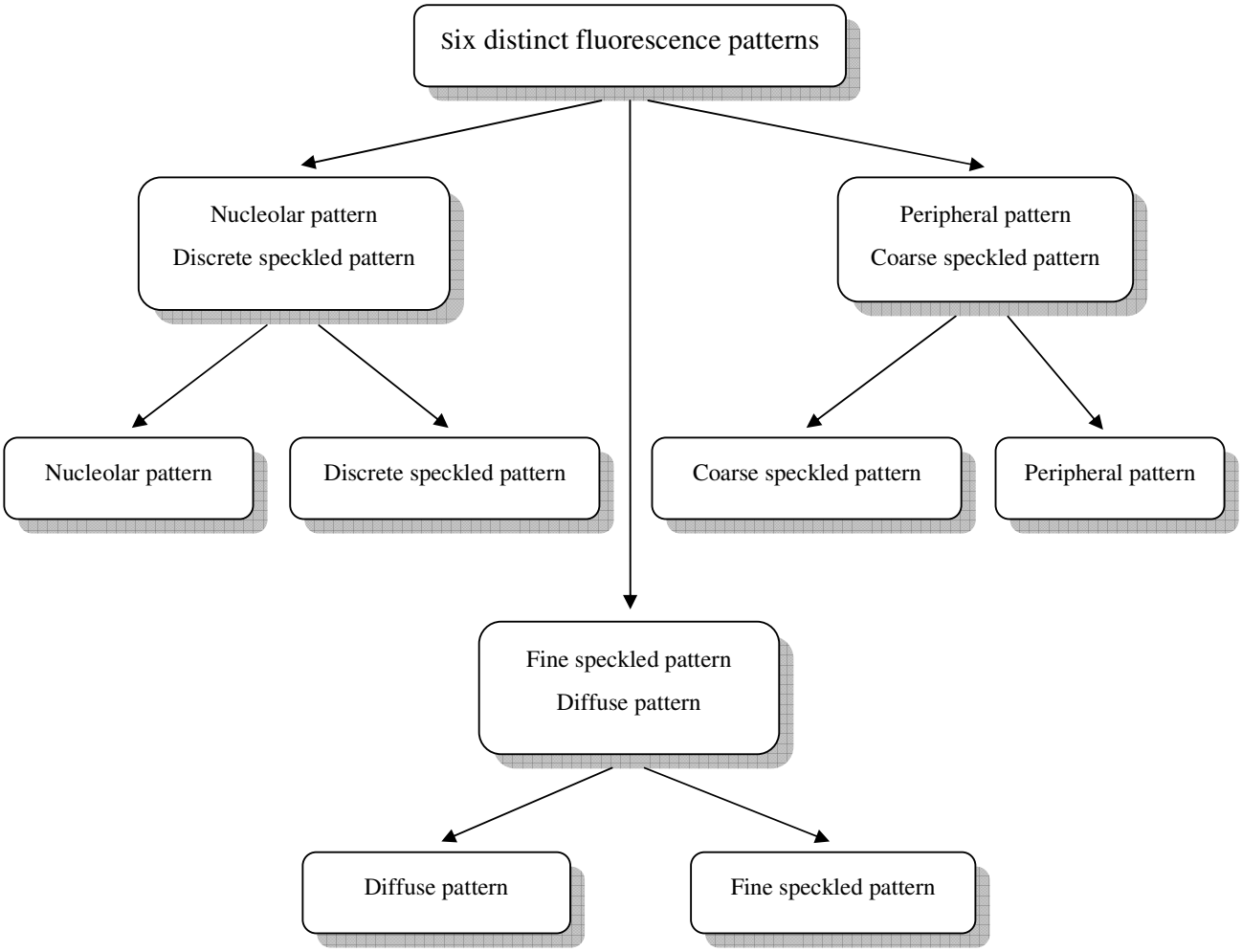


Fig. 7. The flowchart of the pattern classification

### 3.3 RESULT

This study totally experimented fluorescence patterns which from 158 IIF images (including 8 images of diffuse pattern and 30 images of others patterns) to verify the

accuracy of the proposed method. This work presented a practical method for automatically classify outlines of fluorescence pattern in IIF images. After image analysis, there were four features utilized to identify fluorescence patterns, which were the gray-level threshold, an Euler number, disorders and the ratio of cell gray-level. Then the decision tree was utilized to distinguish these images automatically with above-mentioned features as described.

Table 2 lists the classification results of the proposed method. The average accuracy of the total patterns is eighty seven per centum. In the six different patterns, the accuracy of the coarse speckled pattern is eighty six per centum, the diffuse pattern is ninety per centum, the discrete speckled pattern is eighty six per centum, the fine speckled pattern is ninety three per centum, the nucleolar pattern is eighty three per centum and the peripheral pattern is seventy five per centum. All the accuracy of the six patterns is larger than seventy five per centum or equal to seventy five per centum. There was only some cases generated an undesired classification result. This thesis definitely classified recognitions of image that are similarly to those manually classified.

Table 2. The classification results of the proposed method

| Type of pattern | Coarse speckled | Fine speckled | Discrete speckled | Peripheral | Diffuse | Nucleolar |
|---|---|---|---|---|---|---|
| Coarse speckled | 26 | 0 | 0 | 0 | 0 | 0 |
| Fine speckled | 0 | 28 | 3 | 2 | 1 | 3 |
| Discrete speckled | 0 | 0 | 26 | 0 | 0 | 0 |
| Peripheral | 4 | 0 | 0 | 6 | 2 | 2 |
| Diffuse | 0 | 0 | 0 | 0 | 27 | 0 |
| Nucleolar | 0 | 2 | 1 | 0 | 0 | 25 |
| Accuracy | 86.7% | 93.3% | 86.7% | 75% | 90% | 83.3% |

# CHAPTER4

# CONCLUSION

This paper presented a practical method for automatically detecting cell outlines and classification of fluorescence pattern in IIF images. In the detection procedure, the preprocessing enhanced IIF images and the CHT was utilized to produce the outline of the cell automatically. The simulated consequences showed that the proposed method determines the outlines of cells that were very similar to manual sketched ones. Experimental results revealed that the proposed method could precisely detect the outline of fluorescence patterns from IIF images. Besides, the proposed method still obtained an unexpected outlines of the connected region cells as show in Figure 8. But, this situation was rare in ANA testing. Results of this paper obtained the good precision of detection from IIF images.

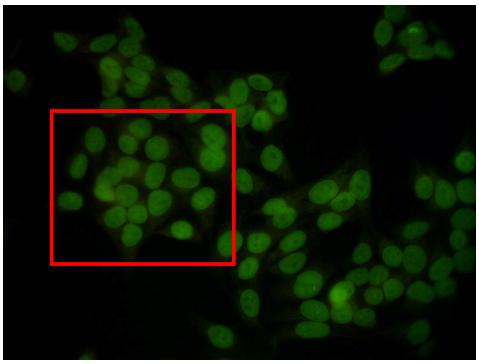

Fig. 8. Cells with a serious overlapping

In the classification, the experiment based on the objective feature measurements gave us new insights into the application. This study proposed a method based on decision tree with four features, i.e. the gray-level threshold, an Euler number, disorders and the ratio of cell gray-level. It totally experimented on 158 autoantibody fluorescence patterns from the detection results. The average accuracy of the total patterns is 0.874. All the accuracy of the six patterns is larger than 0.75 or equal to 0.75. By the results, it can be found that the four features are useful for classification with decision tree. The classifier could decide which the ANA pattern is with the image features of an image. The practicability of the resulting classifier is similar to the expert.

Although this study provided the convince results for detecting and classifying in ANA testing, there were still some parts of the proposed method should be improved in the future. Due to the technique of data acquisition is not skillful, the large number of overlapped cell, the tiny variation between fluorescence cells and background, and the autoantibody fluorescence pattern is very difficult to segment. As long as these problems can be overcoming step by step, the accuracy of the proposed automatic detection will increase than before. Besides, for the classification improvement, developing the texture features will practice to improve the consequences of the classification procedure.

# REFERENCE


[1] Y. Polotsky, J. P. Nataro, D. Kotler, T. J. Barrett, and J. M. Orenstein, "HEp-2 cell adherence patterns, serotyping, and DNA analysis of Escherichia coli isolates from eight patients with AIDS and chronic diarrhea," *Journal of Clinical Microbiology*, vol. 35, no. 8, pp. 1952-1958, Aug.1997.

[2] P. Soda, "Early Experiences in the Staining Pattern Classification of HEp-2 Slides," in *Computer-Based Medical Systems* 2007. CBMS '07. Twentieth IEEE International Symposium on, 2007, pp. 219-224.

[3] P. Soda and G. Iannello, "A Hybrid Multi-Expert Systems for HEp-2 Staining Pattern Classification," in *Image Analysis and Processing* 2007, pp. 685-690.

[4] H. S. Wu and J. Barba, "An Efficient Semiautomatic Algorithm for Cell Contour Extraction," *Journal of Microscopy-Oxford*, vol. 179, pp. 270-276, Sept.1995.

[5] H. S. Wu, J. Barba, and J. Gil, "Iterative thresholding for segmentation of cells from noisy images," *Journal of Microscopy-Oxford*, vol. 197, pp. 296-304, Mar.2000.

[6] H. S. Wu, J. Barba, and J. Gil, "An iterative algorithm for cell segmentation using short-time Fourier transform," *Journal of Microscopy-Oxford*, vol. 184, pp. 127-132, Nov.1996.

[7] Y.L.Huang, Y.L.Jao, T.Y.Hsieh, and C.W.Chung, "Adaptive Automatic Segmentation of HEp-2 Cells in Indirect Immunofluorescence Images," in *Sensor Networks, Ubiquitous and Trustworthy Computing* 2008, pp. 418-422.

[8] Y.L.Huang, C.W.Chung, T.Y.Hsieh, and Y.L.Jao, "Outline Detection for the HEp-2 Cell in Indirect immunofluorescence Images Using Watershed Segmentation," in *Sensor Networks, Ubiquitous and Trustworthy Computing* 2008, pp. 423-427.

[9] W. Hai-Shan, J. Barba, and J. Gil, "A parametric fitting algorithm for segmentation of cell images," *Biomedical Engineering*, vol. 45, no. 3, pp. 400-407, 1998.

[10] W. N. Lie, "Automatic Target Segmentation by Locally Adaptive Image Thresholding," *Image Processing*, vol. 4, no. 7, pp. 1036-1041, July1995.

[11] Y. H. Kim and S. D. Kim, "Image Flow Segmentation and Estimation Using Displaced Spatial Gradient," *Electronics Letters*, vol. 28, no. 24, pp. 2213-2215, Nov.1992.

[12] S. Sarkar and K. L. Boyer, "On Optimal Infinite Impulse-Response Edge-Detection Filters," *IEEE Transactions on Pattern Analysis and Machine Intelligence*, vol. 13, no. 11, pp. 1154-1171, Nov.1991.

[13] D. Hahm and U. Anderer, "Establishment of HEp-2 cell preparation for automated analysis of ANA fluorescence pattern," *Cytometry Part A*, vol. 69A, no. 3, pp. 178-181, Mar.2006.

[14] D. H. Solomon, A. J. Kavanaugh, and P. H. Schur, "Evidence-based guidelines for the use of immunologic tests: Antinuclear antibody testing," *Arthritis & Rheumatism-Arthritis Care & Research*, vol. 47, no. 4, pp. 434-444, Aug.2002.

[15] A. Rigon, P. Soda, D. Zennaro, G. Iannello, and A. Afeltra, "Indirect inununofluorescence in autoimmune diseases: Assessment of digital images for diagnostic purpose," *Cytometry Part B-Clinical Cytometry*, vol. 72B, no. 6, pp. 472-477, Nov.2007.

[16] U. Sack, S. Knoechner, H. Warschkau, U. Pigla, F. Emmrich, and M. Kamprad, "Computer-assisted classification of HEp-2 immunofluorescence patterns in autoimmune diagnostics," *Autoimmunity Reviews*, vol. 2, no. 5, pp. 298-304, Sept.2003.

[17] L. Vincent and P. Soille, "Watersheds in Digital Spaces - An Efficient Algorithm Based on Immersion Simulations," *IEEE Transactions on Pattern Analysis and Machine Intelligence*, vol. 13, no. 6, pp. 583-598, June1991.

[18] S. Suhaila and T. Shimamura, "Power Spectrum tstimation Method for Image Denoising by Frequency Domain Wiener Filter,", 3 ed 2010, pp. 608-612.

[19] N. Otsu, "Threshold Selection Method from Gray-Level Histograms," *IEEE Transactions on Systems Man and Cybernetics*, vol. 9, no. 1, pp. 62-66, 1979.

[20] X.Lin, J.Ji, and Y.Gu, "The Euler Number Study of Image and its Application," in *Industrial Electronics and Applications* 2007, pp. 910-912.

[21] T. J. Atherton and D. J. Kerbyson, "Circle detection using Hough transform filters," in *Image Processing and its Applications* 1995, pp. 370-374.

[22] L. Hoo Cheol, C. Yungeun, K. Young Joong, H. Dae Hie, P. Sin Suk, and L. Myo Taeg, "Vision-Based Estimation of Bolt-Hole Location using Circular Hough transform," 2009, pp. 4821-4826.

[23] P. Perner, "Classification of HEp-2 Cells using Fluorescent Image Analysis and Data Mining," in *Pattern Recognition,* 2 ed 1998, pp. 1677-1679.

[24] P. Sreedevi, W. L. Hwang, and S. Lei, "An Examplar-Based Approach for Texture Compaction Synthesis and Retrieval," *IEEE Transactions on Image Processing*, vol. 19, no. 5, pp. 1307-1318, May2010.

[25] Y. Zhengmao, H. Mohamadian, and I. Majlesein, "Adaptive Enhancement of Gray Level and True Color Images with Quantitative Measurement Using Entropy and Relative Entropy," 2008, pp. 127-131.

[26] K. Shah and V. Gandhi, "Image Classification Based on Textural Features using Artificial Neural Network (ANN)," 2004.

[27] A. Abdelhalim and I. Traore, "A New Method for Learning Decision Trees from Rules," 2009, pp. 693-698.

[28] M. Moussa, J. Ruwanpura, and G. Jergeas, "Decision tree modeling using integrated multilevel stochastic networks," *Journal of Construction Engineering and Management-Asce*, vol. 132, no. 12, pp. 1254-1266, Dec.2006.

[29] M. Moussa, J. Y. Ruwanpura, and G. Jergeas, "Decision tree module within decision support simulation system," 2004, pp. 1268-1276.

[30] D. Haizhou and M. Chong, "Study on constructing generalized decision tree by using DNA coding geneticalgorithm," 2009, pp. 163-167.